

# Localization, Dynamics, and Protein Interactions Reveal Distinct Roles for ER and Golgi SNAREs

Jesse C. Hay,\* Judith Klumperman,‡ Viola Oorschot,‡ Martin Steegmaier,\* Christin S. Kuo,\* and Richard H. Scheller\*

\*Howard Hughes Medical Institute, Department of Molecular and Cellular Physiology, Stanford University School of Medicine, Stanford, California 94305-5428; and ‡Medical School, University of Utrecht, 3584CX Utrecht, The Netherlands

**Abstract.** ER-to-Golgi transport, and perhaps intraGolgi transport involves a set of interacting soluble *N*-ethylmaleimide-sensitive factor attachment protein receptor (SNARE) proteins including syntaxin 5, GOS-28, membrin, rsec22b, and rbet1. By immunoelectron microscopy we find that rsec22b and rbet1 are enriched in COPII-coated vesicles that bud from the ER and presumably fuse with nearby vesicular tubular clusters (VTCs). However, all of the SNAREs were found on both COPII- and COPI-coated membranes, indicating that similar SNARE machinery directs both vesicle pathways. rsec22b and rbet1 do not appear beyond the first Golgi cisterna, whereas syntaxin 5 and membrin penetrate deeply into the Golgi stacks. Temperature shifts reveal that membrin, rsec22b, rbet1, and syntaxin 5 are present together on membranes that rapidly recy-

cle between peripheral and Golgi-centric locations. GOS-28, on the other hand, maintains a fixed localization in the Golgi. By immunoprecipitation analysis, syntaxin 5 exists in at least two major subcomplexes: one containing syntaxin 5 (34-kD isoform) and GOS-28, and another containing syntaxin 5 (41- and 34-kD isoforms), membrin, rsec22b, and rbet1. Both subcomplexes appear to involve direct interactions of each SNARE with syntaxin 5. Our results indicate a central role for complexes among rbet1, rsec22b, membrin, and syntaxin 5 (34 and 41 kD) at two membrane fusion interfaces: the fusion of ER-derived vesicles with VTCs, and the assembly of VTCs to form *cis*-Golgi elements. The 34-kD syntaxin 5 isoform, membrin, and GOS-28 may function in intraGolgi transport.

**M** AINTENANCE of the differentiated membrane compartments in cells requires precise control of intracellular membrane fusion reactions. Fusion of transport vesicles with target membranes allows directed movement of proteins, lipids, and cellular messengers between organelles while maintaining the metabolic integrity of both the donor and acceptor compartments. Several classes of proteins have been identified that mediate aspects of cargo recruitment and vesicle formation, targeting, and fusion. One class of vesicle-trafficking proteins, referred to as soluble *N*-ethylmaleimide sensitive factor attachment protein receptors (SNAREs),<sup>1</sup> pro-

teins of the vesicle-associated membrane protein (VAMP) and syntaxin families, may impart a component of the specificity to membrane fusion reactions through their compartment-specific localizations and protein interactions. Vesicle and target membrane SNAREs form tight oligomeric protein complexes proposed to direct membrane fusion (Söllner et al., 1993; Bennet and Scheller, 1993; Pevsner et al., 1994; Weber et al., 1998). Formation of SNARE complexes appears to be highly cooperative, since binding of one protein can greatly potentiate binding of another (Pevsner et al., 1994; Hayashi et al., 1994; Stone et al., 1997).

The mechanism of ER-to-Golgi transport has remained particularly elusive since specific roles have not yet been assigned to the five or more interacting ER/Golgi SNARE proteins. Our study (Hay et al., 1997) showed that immunoprecipitation of one ER/Golgi SNARE from rat liver membrane extracts, syntaxin 5 (Hardwick and Pelham, 1992; Bennet et al., 1993), resulted in coprecipitation of rbet1 (Hay et al., 1996; Zhang et al., 1997), rsec22b (Hay et al., 1996; Paek et al., 1997), membrin (Hay et al., 1997; Lowe et al., 1997), and Golgi SNARE of 28 kD (GOS-28; Subramaniam et al., 1996; Nagahama et al., 1996). Al-

Jesse C. Hay and Judith Klumperman contributed equally to this paper. The present address of Jesse C. Hay is Department of Biology, University of Michigan, 830 N. University, Ann Arbor, MI 48109-1048.

Address correspondence to Richard H. Scheller, Howard Hughes Medical Institute, Department of Molecular and Cellular Physiology, Stanford University School of Medicine, Stanford, CA 94305-5428. Tel.: 650-723-9075; FAX: 650-725-4436; E-mail: scheller@cmgm.stanford.edu

1. *Abbreviations used in this paper.* IC, intermediate compartment; SNARE, soluble *N*-ethylmaleimide-sensitive factor attachment protein receptor; VTC, vesicular tubular cluster.

though these five proteins are coisolated from detergent extracts, little is known about the pattern of interactions among them, since coisolations from cell extracts (Hay et al., 1997; Sogaard et al., 1994) may involve a series of partially overlapping subcomplexes rather than a single complex containing all of these SNAREs. In addition, it is not known which proteins are included in the complex(es) by virtue of direct interactions with syntaxin 5, as opposed to indirect interactions mediated through other proteins. Several direct interactions have been observed among the potential yeast homologs of the ER/Golgi SNAREs (Stone et al., 1997; Sacher et al., 1997), but these have not yet been correlated with specific vesicle types or dynamics.

Progress has been made in identifying vesicle pathways in ER/Golgi transport through characterization of the vesicle coat complexes that mediate aspects of cargo selection and vesicle budding (Kuehn and Schekman, 1997; Cosson et al., 1997; Schekman and Mellman, 1997). COP II coats mediate budding from the ER and at least the initial stage of transport to the Golgi (Kuehn and Schekman, 1997; Rowe et al., 1996). COP I vesicles, on the other hand, are involved in retrograde retrieval from the intermediate compartment (IC) and Golgi back to the ER (Letourneur et al., 1994). Other data support an additional role for COPI in anterograde movement (Rowe et al., 1996; Orci et al., 1997), possibly acting after COPII (Rowe et al., 1996; Scales et al., 1997). ER/Golgi transport may also involve other uncharacterized coat complexes, since COP II-homologous genes are apparent in the yeast genome (Kuehn and Schekman, 1997). Studies on transport from the ER to the Golgi emphasize the importance of movement of larger polymorphic elements of the IC referred to as vesicular tubular clusters (VTCs). By electron microscopy, VTCs are observed to be either Golgi-adjacent or peripheral (Bannykh et al., 1996). Golgi-adjacent VTCs form a dense cluster some have referred to as the *cis*-Golgi network in the juxtannuclear region, making them difficult to resolve from Golgi by light microscopy. Peripheral VTCs, on the other hand, are scattered throughout the cell, and are readily differentiated from Golgi by light microscopy. These peripheral clusters are surrounded by budding, or exit sites located on rough ER tubules. From these peripheral sites, VTCs appeared to mediate transport of vesicular stomatitis virus (VSV) G protein through large expanses of cytoplasm to the Golgi complex (Presley et al., 1997; Scales et al., 1997), perhaps traveling along microtubule tracks. Mobile VTCs contain both COP I and COP II coats, blurring the functional distinction between these complex membrane structures and small coated transport vesicles. Incorporation of specific SNARE proteins and protein complexes into models of coat protein function would provide a firm mechanistic basis for the functional proposals. In fact, these two families of vesicle-trafficking proteins must act in concert to form and deliver vesicles, as illustrated by their coprecipitation from extracts of forming ER-derived transport vesicles (Kuehn et al., 1998).

Further characterization of ER/Golgi SNARE complexes between more precisely known subsets of proteins must be accompanied by a morphological understanding of the subcellular localization and dynamics of each of the participant SNAREs. What are the steady-state distributions of each SNARE in the ER, IC, and Golgi? Which of

the ER/Golgi SNAREs cycle rapidly between ER and Golgi, and which remain more or less stationary? Do distinct subsets of SNARE proteins reside on COPI and COPII vesicles, thus specifying distinct destinations? By combining immunoelectron microscopy with immunofluorescence, subcellular fractionation, immunoprecipitation and yeast two-hybrid analysis, we here begin to define the specific compartmental localizations, dynamics, and interactions of the five ER/Golgi SNAREs: syntaxin 5, rbet1, rsec22b, membrin, and GOS-28. In contrast to preliminary EM analyses (Paek et al., 1997; Banfield et al., 1994), we use specific antibodies to detect endogenous SNARE proteins at steady state, without recombinant or tagged expression. We establish distinct yet overlapping trafficking patterns for rsec22b, rbet1, membrin, and syntaxin 5, and distinct protein interactions for the two isoforms of syntaxin 5. The localizations and pattern of protein interactions among these proteins suggest that functionally distinct protein complexes are spatially and temporally segregated in ER and Golgi transport.

## Materials and Methods

### Antibodies

Rabbit antisera for msec13 (Tang et al., 1997), calnexin (Hammond and Helenius, 1994), rbet1 (Hay et al., 1997), syntaxin 5 (Hay et al., 1996), and a mouse monoclonal for GOS-28 (Subramaniam et al., 1996) have been previously described. A rabbit antibody to  $\beta$ -COP raised against the EAGE peptide (Duden et al., 1991) was a gift of Dr. Suzanne Pfeffer (Stanford University). Identical labeling patterns were obtained with antibodies raised against the same epitope, and were kindly forwarded by Dr. Irina Majoul and Dr. Jennifer Lippincott-Schwartz (National Institutes of Health). Anti-p58 was from Drs. Ralf Pettersson and Ulla Lahtinen (Ludwig Institute, Stockholm, Sweden). Immunofluorescence staining of syntaxin 5 was also carried out using a rabbit antiserum kindly provided by Dr. Bill Balch (Scripps Institute, La Jolla, CA). Rabbit antisera against mouse sec22b and rat membrin were raised by subcutaneous injection of bacterially expressed hexahistidine-tagged fusion proteins using Freund's adjuvant. The expression constructs included msec22b amino acids 2-195 and membrin amino acids 2-125. The rabbit antibodies were affinity-purified using bead-immobilized msec22b and membrin fusion proteins, respectively. The purified antibodies were eluted from affinity columns using 0.1 M glycine (pH 2.5), neutralized, and stored at 4°C in the presence of 0.05% azide. Mouse monoclonal antibodies against rbet1 were prepared by intraperitoneal injection of purified soluble bacterially expressed rbet1 (amino acids 2-95) produced as a glutathione-S-transferase (GST)-rbet1 fusion protein, and then thrombin-cleaved and separated from GST. Hybridoma production, ELISA screening, subcloning, expansion, and storage of cell lines were carried out by well-established methods (Harlow and Lane, 1988). Monoclonal antibodies 16G6 and 4E11 were affinity-purified using bead-immobilized recombinant rbet1. Routine Western immunoblotting experiments were carried out using ECL (Amersham Corp., Arlington Heights, IL) and autoradiography.

### Immunogold Labeling of Ultrathin Cryosections

Subcellular localizations of the endogenous SNARE proteins were studied on ultrathin cryosections of PC12 and HepG2 cells (see Figs. 2-5) and exocrine pancreas, COS, and NRK cells (not shown). Cells and tissue were fixed in 2% formaldehyde and 0.2% glutaraldehyde in 0.1 M phosphate buffer, pH 7.4, and prepared for cryosectioning and double immunogold labeling as described (Slot et al., 1991) with the slight modification that sections were picked up in a 1:1 mixture of methyl cellulose and 2.3 M sucrose, which results in an improved ultrastructure (Liou et al., 1996). The best results were obtained with affinity-purified polyclonal rabbit antibodies against rsec22b, membrin, and syntaxin 5, and with culture medium from the mouse hybridoma 16G6 against rbet1, all at a dilution of 1:10. For GOS-28 (monoclonal HFD9), no specific labeling was obtained. Labeling density for a specific SNARE differed considerably between cell

types. In PC12 cells, all SNARE proteins exhibited a high yield of labeling, and therefore all quantitative and double-labeling studies were carried out in these cells. For a quantitative analysis of the subcellular distributions of the ER/Golgi SNAREs (Table I), a high-quality section was selected at low magnification. Subsequently, the section was scanned systematically at 25,000 $\times$ . All gold particles within a distance of 30 nm of a membrane were allocated to that type of membrane. About 90–98% of all gold particles were found over membranes of the ER, IC, and Golgi complex. The number of gold particles found over a specific compartment was then expressed as the percentage of total gold. For each SNARE protein, at least three EM grids were analyzed in this manner, and all quantitations were carried out in cells double-labeled for COPII. Since in ultrathin sections putative connections of COPII-coated buds with the ER are not always visible, for the quantitative analyses all COPII-coated membranes were considered part of the IC. The data in Table I summarizes the results of the different counting sessions, with about 150–200 gold particles counted per session.

In a separate experiment, the *cis-trans* distribution of membrin and syntaxin 5 over the Golgi complex was determined (Table II). About 25 Golgi complexes with a clear *cis*→*trans* polarity were selected. The number of gold particles found over the individual cisternae, numbered G1→G5 from *cis* to *trans*, was expressed as a percentage of the total number of gold particles present on the Golgi complexes.

To determine the relative enrichment of the ER/Golgi SNAREs on COPI- vs. COPII-coated membranes of the IC, double-labeling experiments for each SNARE with COPI or COPII were performed. In each counting session, at least 50 random IC membrane profiles that were positively stained for the SNARE protein were scored positive or negative for COPI or COPII. Tubular membrane profiles were scored positive for colocalization only if the SNARE gold particle was within a distance of 40 nm from the COPI or COPII gold particle. Quantitations of a specific combination of antibodies were carried out in at least four counting sessions, all on different EM grids. The number of SNARE-positive IC profiles that contained colocalizing COPI or COPII was expressed as the percentage of the total number of SNARE-positive IC profiles analyzed.

### Fluorescence Microscopy

Cell lines were maintained in a 5% CO<sub>2</sub> incubator using routine media formulations. Before 15°C incubations, tissue culture medium was adjusted to 40 mM Hepes, pH 7.4. For 15°C incubations, cells cultured in microscope slide growth chambers (Nunc Inc., Naperville, IL) were placed below the water surface in a 15°C bath. Regardless of incubation temperature, cells were fixed with 4% paraformaldehyde at room temperature for 30 min. Immunostaining and fluorescence microscopy were carried out as described (Hay et al., 1996).

### Subcellular Fractionation

Two 15-cm plates of NRK cells growing at 37°C were buffered to pH 7.4 with 40 mM Hepes and then returned to 37°C or incubated below the surface of a 15°C water bath for 2 h. Cells were chilled on ice and then swollen in 10 mM ice-cold Hepes, pH 7.4, for 3 min. The Hepes was removed and replaced with 0.5 ml of homogenization buffer (Hay et al., 1996), and the cells were scraped from the plate with a no. 7 rubber stopper (sliced in half) and homogenized by five strokes in a Dounce homogenizer (Kontes Glass Co., Vineland, NJ). Nuclei and unbroken cells were removed by centrifugation at 1,000 *g* for 10 min. For the gradients in Fig. 8, A, D, and G, the postnuclear supernatant was adjusted to 0.75 M sucrose and used as the top layer of a 1.2-ml 0.75–1.75 M sucrose gradient in 20 mM Hepes, pH 7.2, 0.1 M KCl, 2 mM EGTA, 2 mM EDTA. The gradients were initially made with seven discrete layers, but diffusion during the overnight spin produced continuous density profiles. After an 18-h centrifugation at 135,000 *g* ( $r_{av}$ ) in a TLS55 rotor (Beckman Instruments, Inc., Fullerton, CA), gradients were fractionated by hand from the top. Each fraction was supplemented with 2  $\mu$ g BSA before precipitation with ice-cold methanol. The concentrated fractions were then electrophoresed, immunoblotted, and quantitated by autoradiography and densitometry. For gradients in Fig. 8, B, C, E, F, H, and I, 300  $\mu$ l of postnuclear supernatant was adjusted to 600  $\mu$ l of 0.75 M sucrose and layered on top of 700  $\mu$ l of 1.125 M sucrose. Centrifugation and fractionation were as above.

### Immunoprecipitations

Affinity-purified antibodies or control rabbit IgG were chemically conjugated to protein A- or G-Sepharose at a concentration of 2 mg antibody per ml packed Sepharose beads (Harlow and Lane, 1988). Rat liver mi-

croosomes were stripped with 1 M KCl and solubilized in 1% Triton X-100 as before (Hay et al., 1997). Liver extract was precleared by incubation overnight with protein A- and G-Sepharose to deplete it of protein A/G- and Sepharose-binding proteins. 400  $\mu$ l of precleared extract was incubated with 10  $\mu$ l 50% antibody-conjugated beads for 3 h at 4°C with agitation. Beads were then washed 3 $\times$  with 400  $\mu$ l of 20 mM Hepes (pH 7.2), 0.1 M KCl, 2 mM EGTA, 2 mM EDTA, 1% Triton X-100 plus protease inhibitors (see Hay et al., 1997), and once with the same buffer containing 0.2% Triton X-100. Immunoprecipitated proteins were eluted from the beads by incubation at room temperature with 1 $\times$  SDS gel loading buffer lacking reducing reagents for 15 min. After removing the beads by centrifugation, the samples were adjusted to 5% 2-mercaptoethanol, boiled 5 min, and electrophoresed on SDS polyacrylamide gels. Electrophoresed proteins were transferred to nitrocellulose and immunoblotted as usual, except that <sup>125</sup>I-labeled secondary antibodies and Phosphor Imaging (Molecular Dynamics, Sunnyvale, CA) were used to quantify the results rather than ECL and autoradiography.

We estimate that the radioactive intensities of the bands detected by phosphor imaging in Fig. 9 are approximately indicative of the molar quantities of the proteins present. When scaled up, precipitations similar to that shown in the first column of Fig. 9 were electrophoresed and stained by Coomassie blue (Hay et al., 1997), and the relative intensities of the stained SNARE bands closely corresponded to the relative Western signals analyzed in Fig. 9.

### Analysis of Protein–Protein Interactions by the Yeast Two-hybrid System

The full-length or partial coding regions of *rsly1*, *rsec22a*, *rsec22b*, *GOS-28*, *rbet1*, *membrin*, *syntaxin 5*, and *SNAP-25* were subcloned into the yeast expression vectors pGBT9 and pGAD424 (Clontech, Palo Alto, CA). The following vectors contain the following inserts: pGBT9/*rsly1* (residues 15–648); pGBT9/*rsec22a*, *msec22b*, *GOS-28*, *rbet1*, and *membrin* and the corresponding pGAD424 constructs contain the complete coding regions of the proteins; pGAD424/*syntaxin 5* and pGBT9/*SNAP-25* also contain the complete rat coding sequence. Yeast strain HF7c (Clontech) was transformed with bait and prey vectors using the lithium acetate method (Schiestl and Gietz, 1989). Transformants were plated on selection plates lacking tryptophan, leucine, and histidine. After 5 d of incubation at 30°C, colonies were inoculated into supplemented minimal medium lacking tryptophan, leucine, and histidine, and were placed into a shaking incubator at 30°C for 44 h. Cultures were diluted 1:1 in fresh supplemented minimal medium lacking tryptophan, leucine, and histidine, and were incubated for 6 h while shaking at 30°C.  $\beta$ -galactosidase assays were performed on yeast extracts as described (Rose and Botstein, 1983).

Additional combinations of binding partners tested include pGBT9/*membrin* in combination with pGAD424/*membrin*, *msec22b*, *GOS-28*, and *rbet1*. pGBT9/*rsec22a* as bait was tested in combination with pGAD424/*msec22b*, *GOS-28*, and *rbet1*. pGBT9/*msec22b* was tested for binding with *msec22b*, *GOS-28*, and *rbet1*. pGBT9/*GOS-28* was tested for binding with pGAD424/*GOS-28* and *rbet1*. Finally, pGBT9/*rbet1* was tested with pGAD424/*rbet1*. None of these combinations resulted in sufficient binding to produce  $\beta$ -galactosidase activity above background.

## Results

### Subcellular Distributions of *rsec22b*, *rbet1*, *Membrin*, and *Syntaxin 5*

Syntaxin 5 *in vitro* assembles with four other SNARE-like proteins: *GOS-28*, *membrin*, *rsec22b*, and *rbet1*. To better understand the subcellular organization of the ER and Golgi SNAREs, we took an immunoelectron microscopy approach. To enable immunogold labeling of the endogenous SNAREs, we produced new antisera to *membrin*, *rsec22b*, and *rbet1*. As shown in Fig. 1, anti-*membrin* and anti-*rsec22b* affinity-purified rabbit antibodies recognized only their specific target antigens in COS, HepG2, NRK, and PC12 cells. Two new mouse monoclonal antibodies to *rbet1*, 16G6, and 4E11 recognized *rbet1* in a rat-specific fashion. Highly specific polyclonal antibodies to *syntaxin 5*

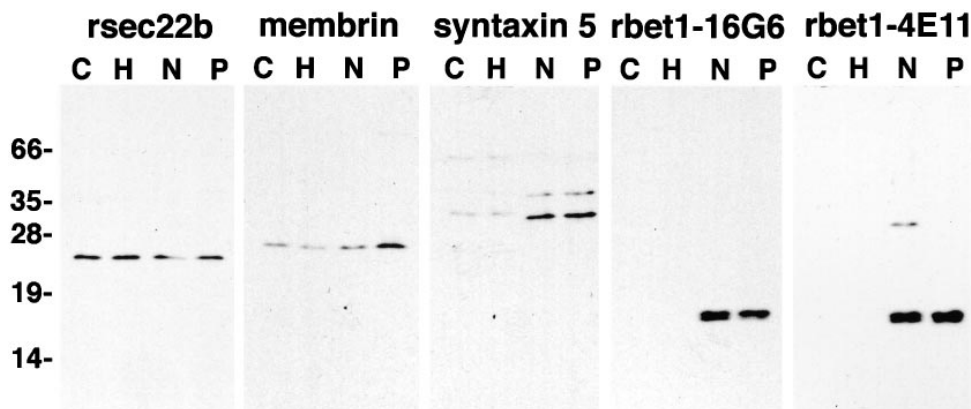


Figure 1. Specific antibodies. COS, HepG2, NRK, and PC12 cells were solubilized in SDS sample buffer, electrophoresed, and transferred to nitrocellulose for immunoblotting with affinity-purified rabbit polyclonal antisera for rsec22b, membrin, and syntaxin 5, or with culture medium from the anti-rbet1 hybridomas 16G6 and 4E11. Molecular masses in kD are indicated on the left.

and rbet1 and a monoclonal antibody for GOS-28 have been described (Hay et al., 1996; Hay et al., 1997; Subramiam et al., 1996).

The subcellular distributions of rsec22b, rbet1, membrin, and syntaxin 5 were established by immunogold labeling of ultrathin cryosections. All four SNARE proteins were detected in the distinct compartments of the early secretory pathway; i.e., the ER, IC, and Golgi. However, quantitative analysis of the labeling patterns obtained in PC12 cells revealed that their relative distribution over these compartments varied. Table I presents the fraction of the total immunoreactivity found in ER, IC, and Golgi. Most of the immunoreactivity for the four proteins investigated (between 65 and 81 percent) was found in membranes characteristic of the IC, whereas labeling over the ER was lower (between 7 and 12 percent). This distribution is consistent with the function of the intermediate compartment as the hub of vesicle trafficking in the early secretory pathway.

Subcellular localization of rsec22b was studied in detail in HepG2 (Fig. 2) and PC12 cells (Fig. 3 A), which gave identical labeling patterns. The majority of label was associated with the IC (Table I, Fig. 2 A). At the ultrastructural level, the IC consists of an elaborate network of vesicular and tubular membrane profiles that appear at distinct sites in the cell both near the Golgi and at the periphery. Many IC clusters, or VTCs, were found to be closely associated with RER cisternae exhibiting COPII-coated membrane buds representing export sites for anterograde cargo. Double-immunogold labeling revealed that rsec22b was often confined to these COPII-coated membranes of the ER and early IC (Fig. 2, A and B).

The labeling pattern obtained for rbet1 was very similar to that of rsec22b (Table I, Fig. 3). Simultaneous labeling of these two SNAREs within the same sections unequivocally

localized them to the same membranes (Fig. 3 A). Membrin showed a more dispersed labeling over the IC than did rsec22b and rbet1, with label extending up to (and within, see below) the Golgi complex (Table I, Fig. 4, A and B). Syntaxin 5 showed a distribution pattern reminiscent of membrin, albeit with higher levels present in the Golgi (Table I, Fig. 5). Within the early membranes of the IC, syntaxin 5 colocalized with rbet1 and rsec22b (Fig. 5 A, inset) to the same membrane profiles.

While only a small percentage of rbet1 and rsec22b is found in the Golgi—6.3% and 8.7%, respectively—20% of membrin and 28% of syntaxin 5 are Golgi-localized. Within the Golgi, the rbet1 and rsec22b immunoreactivity, when present, was restricted to the *cis*-most cisterna (Figs. 2 C and 3 A). In contrast, both membrin and syntaxin 5 show significant immunoreactivity as far into the Golgi as the *trans* cisterna (Figs. 4 B and 5 B). A detailed analysis of the intraGolgi distribution of these latter two SNAREs revealed that membrin was mainly localized to the *cis* and medial cisternae, whereas equal amounts of syntaxin 5 were present in all but the *trans*-most cisternae (Table II).

To determine whether the ER/Golgi SNAREs displayed specificity for the characterized COPI and COPII vesicle pathways in the IC, we performed double-immunogold labelings with COPI (Figs. 2 B, 3 C, and 4 C; COPI is represented by  $\beta$ -COP) and COPII (Fig. 2, A and C, Fig. 3 B, and Fig. 5 A, COPII is represented by msec13). A quantitation of these analyses is presented in Table III. For this analysis we scored as positive only individual membrane profiles, including vesicles as well as larger tubular membranes, to which both sizes of gold particles colocalized. If a membrane was only partially coated, the structure was scored positive for colocalization only if the SNARE-representing gold particle was within a distance of 40 nm of the COP-representing gold particle. rbet1 and rsec22b were particularly enriched in COPII-coated structures (25% colocalization: Fig. 2, A and C, Fig. 3 B, Table III), consistent with their playing an important role on COPII-coated vesicles that are known to bud from the ER (Kuehn and Schekman, 1997), and are involved in the formation of peripheral VTCs (Rowe et al., 1998). All four SNAREs tested were present on COPI-coated membranes (Figs. 2 B, 3 C, and 4 C, Table III).

In summary, these data show that rsec22b and rbet1 have identical distribution patterns and localize preferentially to the early membranes of the IC, whereas membrin

Table I. Relative Distributions of SNARE Proteins Over Compartments of the Early Secretory Pathway in PC12 Cells

	Percentage of Total Gold Particles $\pm$ SD		
	ER	IC	Golgi
rbet1	12.3 $\pm$ 4.5	81.3 $\pm$ 4.0	6.3 $\pm$ 2.1
rsec22b	11.3 $\pm$ 1.2	80.3 $\pm$ 2.5	8.7 $\pm$ 0.9
membrin	9.0 $\pm$ 1.6	71.0 $\pm$ 1.7	20.0 $\pm$ 0.1
syntaxin 5	7.3 $\pm$ 1.9	65.0 $\pm$ 4.1	28.3 $\pm$ 2.4

Quantifications were carried out in three (rsec22b, rbet1, membrin) or four (syntaxin 5) EM grids.

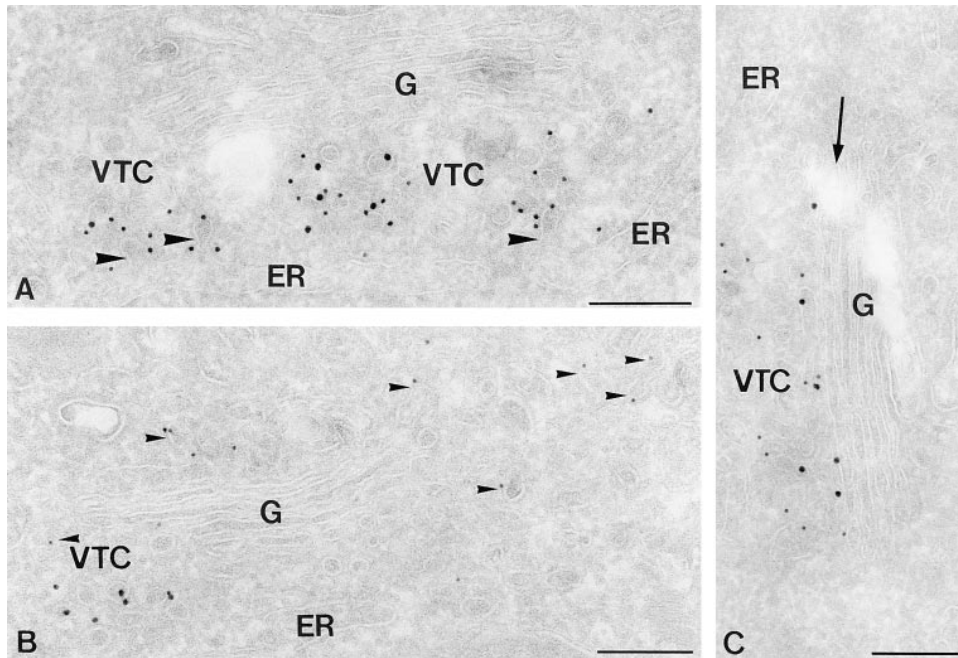


**Figure 2.** Ultrathin cryosections of HepG2 cells showing the subcellular distribution of human sec22b (hsec22b). (A and C) Double immunogold labeling for hsec22b (15 nm gold) and COPII (10 nm gold). hsec22b colocalizes to a high extent with COPII to VTC membranes. Label in the Golgi (G), if detectable, is restricted to the *cis*-most cisterna (arrow in C). Note that the membrane buds evolving from the ER (large arrowhead in A) are coated with COPII. (B) Double immunogold labeling for hsec22b (15 nm gold) and COPI (10 nm gold). COPI-coated membranes (small arrowheads) show a much more widespread distribution than hsec22b-positive membranes. Bars, 200 nm.

and syntaxin 5 have a more widespread distribution including the Golgi. All four SNAREs tested were detected in both COPII and COPI-coated membranes, consistent with the possibility that both of these vesicle types involve similar SNARE machinery.

**Low-temperature Incubations Distinguish Static from Rapidly Cycling ER/Golgi SNAREs**

Immunofluorescence subcellular localization of this set of proteins in NRK cells revealed that all five proteins most intensively stained the juxtannuclear Golgi area under con-

trol steady-state conditions (Fig. 6, first column; 37°C). This finding is consistent with the ultrastructural studies (Table I) since IC elements, which contain the majority of syntaxin 5, membrin, rsec22b, and rbet1, are most concentrated in the Golgi area and are in fact indistinguishable from the Golgi at the light level. GOS-28 appeared perhaps most tightly Golgi-localized, consistent with previous ultrastructural studies (Subramaniam et al., 1995; Nagahama et al., 1996). rsec22b and rbet1 occasionally displayed a distinctly spotty localization reminiscent of peripheral VTCs (Saraste and Svensson, 1991); however, most staining was juxtannuclear.

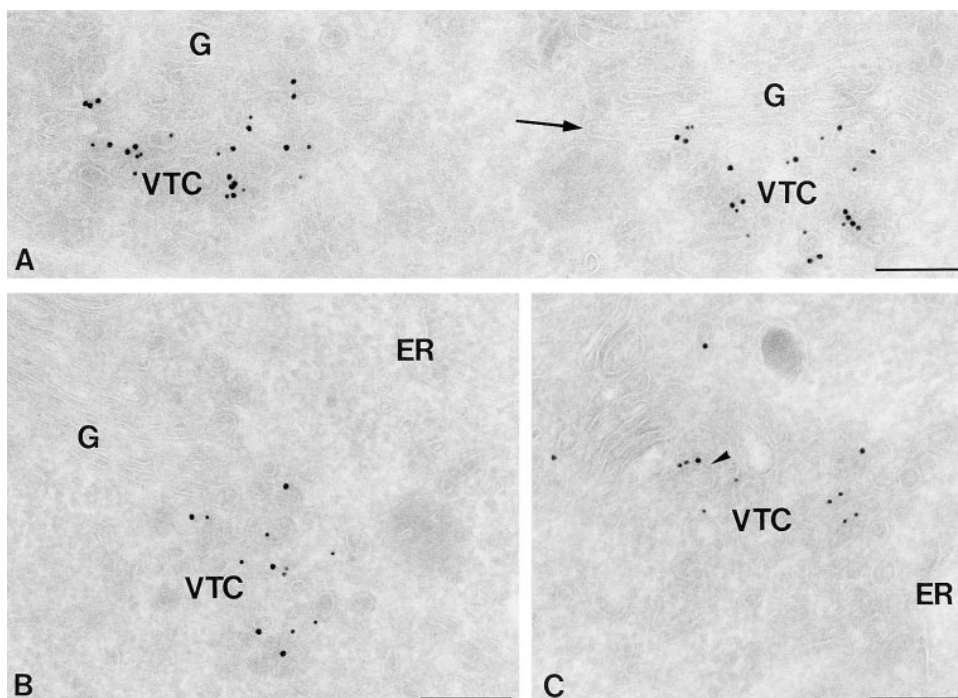


**Figure 3.** Ultrathin cryosections of PC12 cells showing the localization of rbet1. (A) Double immunogold labeling for rsec22b (10 nm gold) and rbet1 (15 nm gold). Both SNARE proteins localize to the same VTC membranes. Label in the Golgi (G) is restricted to the *cis*-most cisterna (arrow). (B) Double immunogold labeling for rbet1 (10 nm gold) and COPII (15 nm gold) showing colocalization on VTC membranes. (C) Double immunogold labeling of rbet1 (10 nm gold) and COPI (15 nm gold). The arrowhead points to a tubular VTC membrane that contains rbet1, and is coated with COPI. Bars, 200 nm.

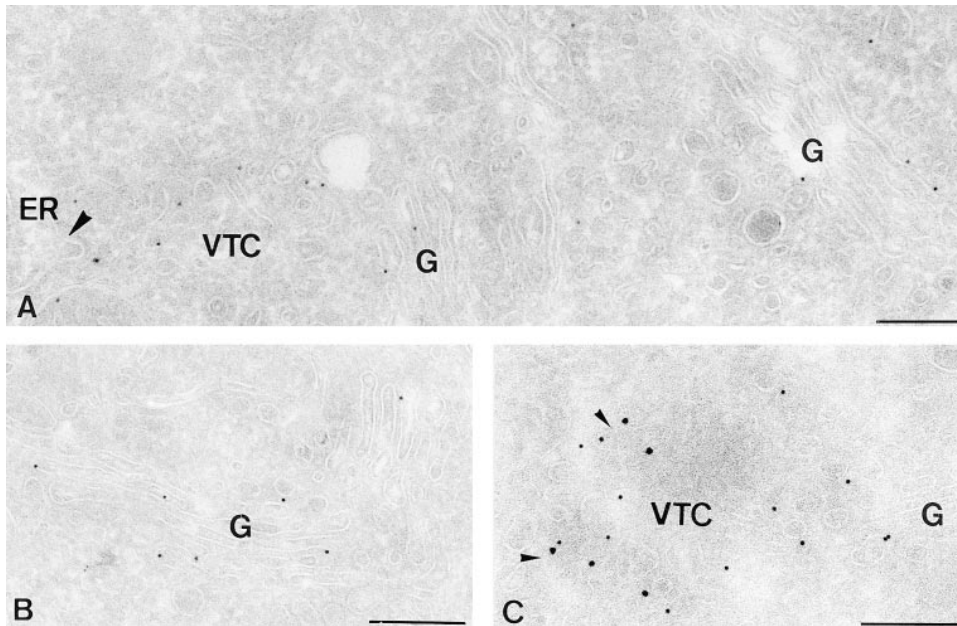


**Figure 4.** Ultrathin cryosections of PC12 cells showing the subcellular localization of membrin. (A and B) Immunogold labeling of membrin (10 nm gold) is dispersed over VTC membranes and the Golgi stack (G). The large arrowhead in A points to a membrane bud on the ER. (C) Double immunogold labeling of membrin (15 nm gold) and COPI (10 nm gold) showing partial colocalization (small arrowheads) on VTC membranes. Bars, 200 nm.

Colocalization of syntaxin 5, GOS-28, membrin, rsec22b, and rbt1 in the Golgi area under steady-state conditions provides no information on differences in their intracellular dynamics. For example, several of the proteins may operate itinerantly, traveling with cargo from the ER to Golgi and then recycling back for reuse while others may reside relatively statically on the Golgi or preGolgi elements. To compare intracellular dynamics of the proteins, normal rat kidney cells were incubated at 15°C, a temperature at which transport from the ER to Golgi is slowed dramatically, resulting in accumulation of vesicle compo-

nents and cargo in peripheral VTCs (Saraste and Svensson, 1991; Matlin and Simons, 1983; Kuismanen and Saraste, 1989). As shown in Fig. 6, upon shift from 37°C to 15°C, the membrin distribution shifts to a much more peripheral spotty pattern. At 15°C, membrin is present in variously sized and shaped cytoplasmic foci, indicative of peripheral VTCs. Based on the observation that the membrin juxtannuclear staining deintensifies as the peripheral staining intensifies, it seems likely that retrograde transport continues at 15°C while anterograde movement is greatly slowed, resulting in a net shift of the steady-state

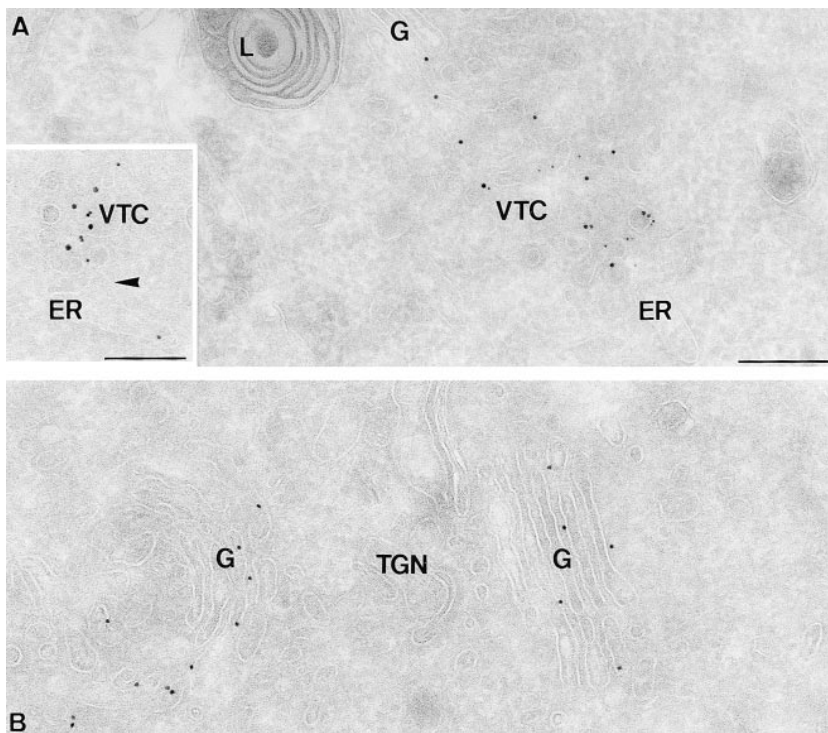


**Figure 5.** Ultrathin cryosections of PC12 cells showing immunogold labeling of syntaxin 5. (A) Syntaxin 5 (10 nm gold) partially colocalizes with COPII (5 nm gold) on VTC membranes. The inset shows rsec22b (10 nm gold) and syntaxin 5 (15 nm gold) colocalization in membrane profiles of a VTC that is in close proximity to the ER (arrowhead points to an ER membrane bud). (B) Syntaxin 5 (10 nm gold) is present throughout the entire Golgi stack (G). L, lysosome, TGN, trans Golgi network. Bars, 200 nm.

**Table II. Relative Distributions of SNARE Proteins Over *cis* to *trans* Cisternae (G1 → G5) of the Golgi Complex in PC12 Cells**

SNARE*	Percentage of Total Golgi Gold Particles				
	G1	G2	G3	G4	G5
membrin	39	35	12	12	3
syntaxin 5	22	27	24	20	7

G1 represents the *cis*-most cisternae, which characteristically consists of several discontinuous membranes. G5, the *trans*-most cisternae, was only occasionally observed. About 25 Golgis were analyzed for each protein. \*rsec22b and rbet1 were rarely seen beyond G1, and were not included in this analysis because of difficulty in obtaining a large enough sample of Golgi-localized rsec22b and rbet1.

localization from Golgi adjacent to peripheral VTCs. This redistribution also occurs in the presence of cyclohexamide (not shown), indicating that new membrin synthesis cannot account for intensifying peripheral sites. In the same set of cells, a resident Golgi protein, mannosidase II, remains statically in the Golgi as expected (not shown). Double-labeling between syntaxin 5 and rbet1 (Fig. 6, *second and third rows*) reveals that both of these proteins shift to peripheral VTCs when incubated at 15°C; however, syntaxin 5 appears to redistribute more slowly and less dramatically than rbet1. After 15 min at 15°C, syntaxin 5 exhibits a punctate staining pattern typical for peripheral clusters; however, these peripheral elements are relatively weak compared with the strong juxtannuclear staining. After 60 min, syntaxin 5 is more apparent in peripheral VTCs, but retains relatively strong juxtannuclear staining. The apparent partial commitment of syntaxin 5 to cycling VTCs may be a result of a pool of this protein that remains in the Golgi (see below and Figs. 8 and 9). A double-labeling between GOS-28 and rsec22b (Fig. 6, *bottom two rows*) reveals a dramatic difference in dynamics: throughout a 1-h 15°C incubation, GOS-28 remains statically in a relatively tight juxtannuclear pattern, whereas in the same cells, rsec22b rapidly concentrates in peripheral foci. These immunofluorescence images document a fundamental difference between the life cycles of GOS-28, on the one hand, which remains relatively statically localized, and rbet1, membrin, rsec22b, and syntaxin 5 on the other, which appear to be rapidly moving between peripheral and Golgi-centric sites.

Do the rapidly cycling proteins follow the same pathway? To look for potential differences in their recycling pathways, we performed double-label immunofluorescence comparisons among rbet1, rsec22b, and membrin,

**Table III. Occurrence of SNARE Proteins in COPI and COPII Coated Membranes in PC12 Cells**

	Percentage of Colocalization ± SD	
	COPI	COPII
rbet1	12.5 ± 1.7	25.0 ± 3.0
rsec22b	10.5 ± 3.8	25.0 ± 0.7
membrin	14.0 ± 2.9	10.0 ± 4.0
syntaxin 5	13.0 ± 2.2	7.5 ± 4.0

Ultrathin cryosections were double immunogold-labeled for a SNARE and either COPI or COPII. Numbers indicate the percentage of SNARE-positive IC profiles displaying colocalization of a SNARE with COPI or COPII. For each SNARE, at least 200 SNARE-positive IC profiles were analyzed.

when arrested in peripheral VTCs. As shown in the top two panels of Fig. 7, the distributions of rbet1 and rsec22b at 15°C were very similar in double-labeled cells, with intense staining of VTCs. Significantly, in almost all instances both proteins were present in the same individual VTCs (Fig. 7, *arrows*), implying that rsec22b and rbet1 share a very similar recycling pathway. Notably, both proteins exhibited weak tubular/reticular ER staining (Fig. 7, *arrowhead*). Membrin and rbet1 antibodies also clearly labeled the same individual peripheral VTCs (Fig. 7, *bottom two panels*), indicating that these three dynamic SNAREs recycle together on the same VTCs. However, the membrin staining was very focused in the perinuclear area and peripheral VTCs, but was not apparent in the ER. Hence, unlike rsec22b and rbet1, membrin apparently does not cycle fully back through the ER. Alternatively, membrin may recycle through the ER very rapidly, making detection there difficult.

Since changes in antigen accessibility and concentration can potentially affect immunofluorescence and EM images, we sought to confirm independently the localization and dynamics of the SNARE proteins by biochemical fractionation of subcellular membranes on sucrose equilibrium gradients. The relative distributions of each SNARE on subcellular membranes was determined on 0.75–1.75 M sucrose gradients (Fig. 8, *A, D, and G*). A comparison of membrin with GOS-28, a protein limited to the Golgi (Subramaniam et al., 1995; Nagahama et al., 1996), demonstrates that these gradients do not resolve IC from Golgi since the bulk of both proteins substantially overlap in fractions 2, 3, and 4 (Fig. 8 *A*). Likewise, the majority of the IC marker protein p58 (not shown), syntaxin 5, rsec22b, and rbet1 also fall in fractions 2, 3, and 4 (Fig. 8, *D and G*). These gradients do, however, resolve IC/Golgi membranes of fractions 2, 3, and 4 from denser ER membranes of fractions 8, 9, and 10, where the ER protein calnexin peaks (Fig. 8 *G*). Hence, comparison of membrin with GOS-28 in Fig. 8 *A* reveals that very little of either of these SNAREs resides in the ER at steady state, consistent with the immunogold and immunofluorescence analyses (Table I, Figs. 6 and 7). As shown in Fig. 8 *D*, the 41-kD and 34-kD isoforms of syntaxin 5 distribute differently between Golgi/IC and ER membranes, as has been observed before (Hui et al., 1997), with the 41-kD isoform much more relatively enriched in the ER. rsec22b and rbet1 both exhibit a significant steady-state presence in the ER (Fig. 8 *G*), a distribution that is consistent with their apparent enrichment on COPII-coated vesicles that bud from the ER (Table III). The apparent discrepancy in the proportions of rsec22b, rbet1, and syntaxin 5 in the ER as determined by immunogold (Table I) and subcellular fractionation (Fig. 8) may be due to a lower immunogold labeling efficiency in the ER, perhaps due to protein interactions that limit antigen availability. It is also difficult to account for all of the gold particles that label the ER since this compartment is so broadly distributed throughout the cell.

Shallower sucrose gradients were able to resolve membranes of the Golgi and IC partially while pelleting ER. An analysis of membrin and GOS-28 on these gradients confirmed the dramatic difference in these SNAREs' dynamics observed by immunofluorescence. At 37°C, the two proteins resided on IC and Golgi membranes that sub-

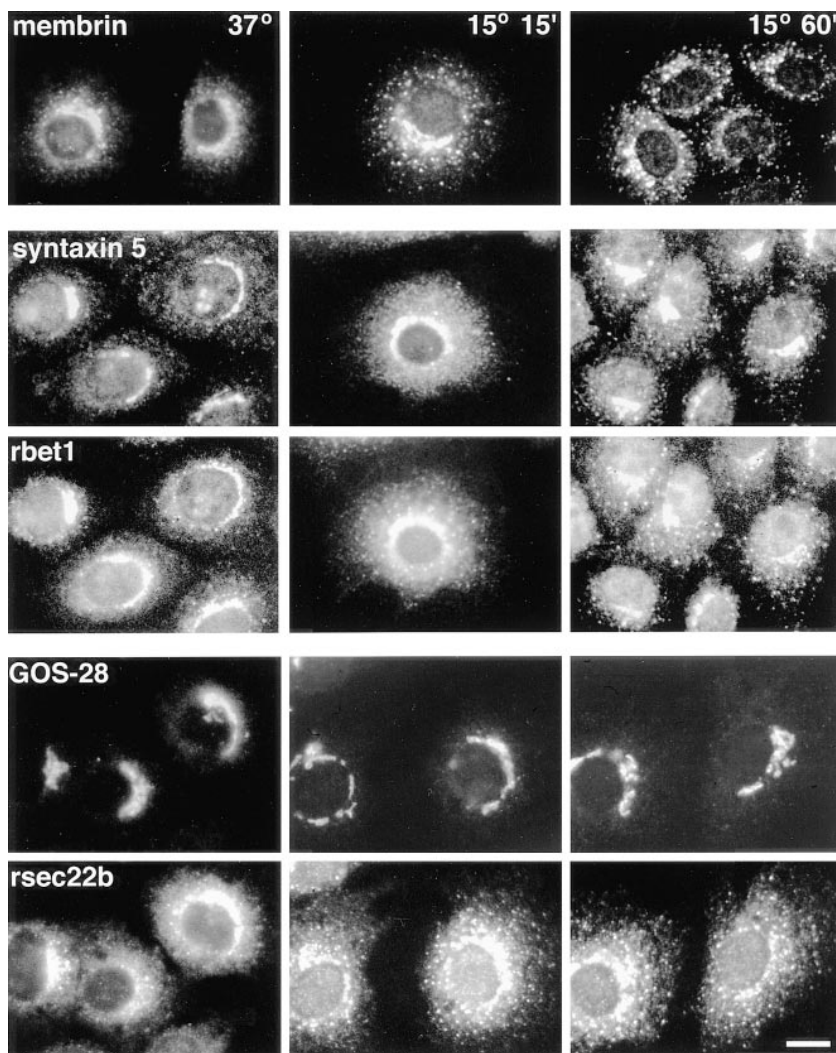


*Figure 6.* The ER/Golgi SNAREs exhibit differing dynamics when incubated at low temperatures. NRK cells incubated at 37°C or 15°C for 15 or 60 min were fixed, permeabilized, and stained for immunofluorescence microscopy with affinity-purified polyclonal (syntaxin 5, rsec22b, membrin) or monoclonal (GOS-28 and rbet1/16G6) antibodies. Panels in the second and third rows from the top represent the same fields of cells, as do panels in the fourth and fifth rows. Bar, 20  $\mu$ m.

stantially overlapped in their densities (Fig. 8 *B*). At 15°C, however, membrin and GOS-28 are noticeably better resolved (Fig. 8 *C*), presumably since membrin accumulates in peripheral VTCs, whereas GOS-28 remains statically in the Golgi (Fig. 6). We speculate that peripheral VTCs unable to migrate from the periphery at 15°C undergo shape, size, and/or content changes that reduce their density, resulting in a shift to lighter gradient fractions. Likewise, the Golgi at 15°C may be altered by the change in trafficking and shifts to fractions of slightly greater density. Other studies have identified accumulated VTCs in a light fraction approximately comigrating with TGN (J. Klumperman, A. Schweizer, H. Clausen, B.L. Tang, W. Hong, V. Oorschot, and H.-P. Hauri, manuscript submitted for publication). Interestingly, at 15°C, syntaxin 5 shifted to IC membranes of lesser density, as did membrin, but also retained a very significant presence on denser membranes containing GOS-28 (Fig. 8, *E* and *F*). This dual trafficking of syntaxin 5 would explain the protein's apparently slower and less complete recruitment to peripheral VTCs observed by immunofluorescence (Fig. 6). Perhaps a pool of Golgi syntaxin 5 is retained in the Golgi by its interactions with GOS-28 (see below). rbet1, rsec22b, and the IC marker p58 (called ERGIC-53 in primates) all displayed

shifting distributions consistent with membrin at 37°C and 15°C (Fig. 8, *H* and *I*). Hence, the immunofluorescence (Figs. 6 and 7) and density gradient (Fig. 8) temperature shift experiments support itinerant cycling functions for rbet1, rsec22b, membrin, and syntaxin 5. In contrast, the relatively static localization of GOS-28 and a portion of syntaxin 5 is consistent with a function that is limited to the Golgi.

#### *Syntaxin 5 Isoforms Participate in Distinct Protein Complexes*

We previously found that two syntaxin 5-associated proteins—rbet1 and GOS-28—were not tightly associated with each other in detergent extracts (Hay et al., 1997), suggesting their presence in distinct mutually exclusive subcomplexes containing syntaxin 5 in common. To help clarify whether other exclusive interactions occur among this group of proteins, we performed immunoprecipitations with eight different polyclonal and monoclonal antisera against ER/Golgi SNAREs, and quantitated coprecipitating proteins by Western blotting using <sup>125</sup>I-labeled secondary reagents and phosphor imaging. As shown in Fig. 9 and Table IV, syntaxin 5, as expected, coprecipi-

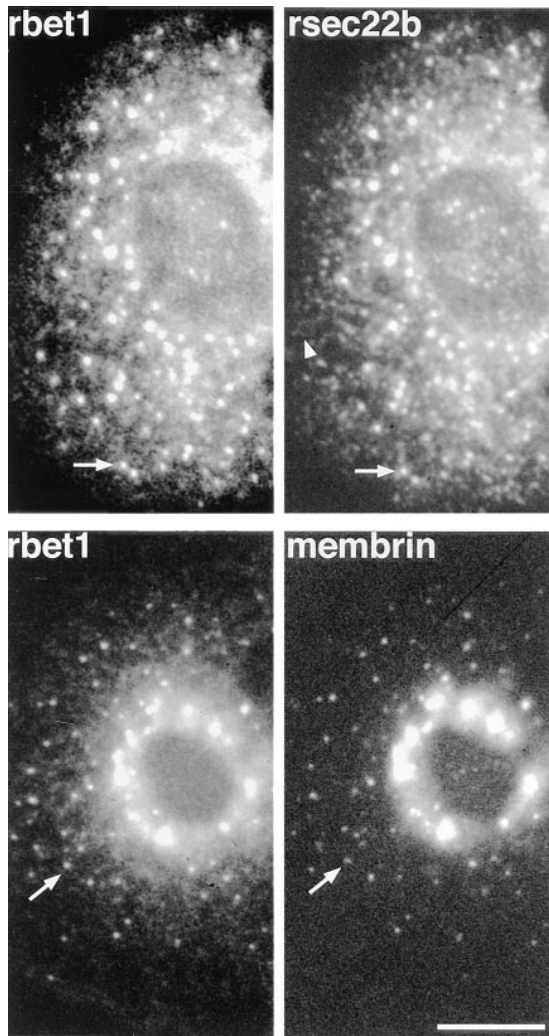


**Figure 7.** Dynamic SNAREs colocalize to the same VTCs. NRK cells were incubated at 15°C for 1 h, fixed, and double-stained for immunofluorescence as in Fig. 6. The arrows indicate individual VTCs clearly visible in both panels. The arrowhead marks tubular/reticular staining characteristic of the ER, a pattern not observed for membrin staining. Bar, 20  $\mu$ m.

tated at least four ER/Golgi SNAREs, including GOS-28, rsec22b, membrin, and rbet1. All of these syntaxin 5-associated proteins reciprocally coprecipitated syntaxin 5, except for rsec22b, which unfortunately was primarily present as a partially degraded form that apparently does not participate in the protein-protein interactions. Hence, rsec22b precipitations did not provide information about protein complexes containing rsec22b.

The most striking feature of the pattern of coprecipitations was the relative isolation of GOS-28 from the other syntaxin 5-associated SNAREs. Although GOS-28 coprecipitated syntaxin 5 in near-stoichiometric amounts, other SNAREs failed to coprecipitate in significant amounts. A small portion of rsec22b coprecipitated as documented earlier (Hay et al., 1997), but this was only 11% of the amount of coprecipitating syntaxin 5. This apparent lack of association of GOS-28 with membrin, rsec22b, and rbet1 does not arise from a peculiarity of the anti-GOS-28 antibody since two different antibodies to membrin and

three different antibodies to rbet1 coprecipitated insignificant or minor amounts of GOS-28 relative to other coprecipitating species. It appears that GOS-28 may be associated with syntaxin 5 in a complex lacking or excluding membrin, rsec22b, and rbet1. Most interestingly, this complex appears to involve primarily the 34-kD Golgi-centric isoform of syntaxin 5, as opposed to the 41-kD isoform or its major breakdown product of 31 kD. This is in contrast to rbet1 and membrin, which precipitate more balanced ratios of syntaxin 5 isoforms. These data suggest a functional difference among the syntaxin 5 isoforms; the 34-kD isoform may perform a distinct function in conjunction with GOS-28 in the Golgi.

Immunoprecipitation of rbet1 and membrin resulted in coprecipitation of stoichiometrically balanced ratios of associated SNAREs other than GOS-28, indicating that major exclusive relationships do not exist among syntaxin 5, rsec22b, membrin, and rbet1. These proteins may associate together simultaneously in a single quaternary complex.

### *Several ER/Golgi SNAREs Interact Directly with Syntaxin 5*

Although four SNARE-like proteins coprecipitate with syntaxin 5 (Hay et al., 1997), the pattern of direct interactions among this group is unknown. We sought to determine which members of the complex may be included in the complex by virtue of direct interactions with syntaxin 5, as opposed to indirect interactions mediated through other proteins. The yeast two-hybrid system was used to detect and quantify interactions between syntaxin 5 (the 34-kD isoform) and seven potential syntaxin 5-binding proteins (Fig. 10). We used two-hybrid constructs containing the full-length SNAREs, including transmembrane domains. Two proteins presumably irrelevant to the syntaxin 5 complex, SNAP-25 and rsec22a, failed to stimulate  $\beta$ -galactosidase activity, consistent with the expectation that these proteins do not bind syntaxin 5. One of the proteins that coprecipitates with syntaxin 5, mouse sec22b, consistently stimulated a small amount of  $\beta$ -galactosidase activity, indicating that although this protein appears to bind syntaxin 5 weakly, other protein interactions may be critical for its inclusion in the syntaxin 5 complex. Four other members of the syntaxin 5 complex: rsl1 (Peterson et al., 1997; Dascher et al., 1996), GOS-28, membrin, and rbet1, all stimulated a relatively large amount of  $\beta$ -galactosidase activity, consistent with the possibility that each of these proteins can directly interact with syntaxin 5 independently of other protein interactions. Combinations of membrin, rsec22a, msec22b, GOS-28, and rbet1 (see Materials and Methods) were also tested for their ability to interact with each other in the two-hybrid system. No combinations were found to stimulate  $\beta$ -galactosidase activity above background levels. It is possible that pairwise interactions between these proteins are not of sufficient affinity to give a positive signal in the two-hybrid assay; however, the proteins may bind to each other in the context of higher order complexes. The two-hybrid studies delineating the pattern of interactions among this set of proteins limit the possible configurations of SNAREs that determine trafficking pathways in ER/Golgi transport, and help suggest supramolecular models of transport. However, since many

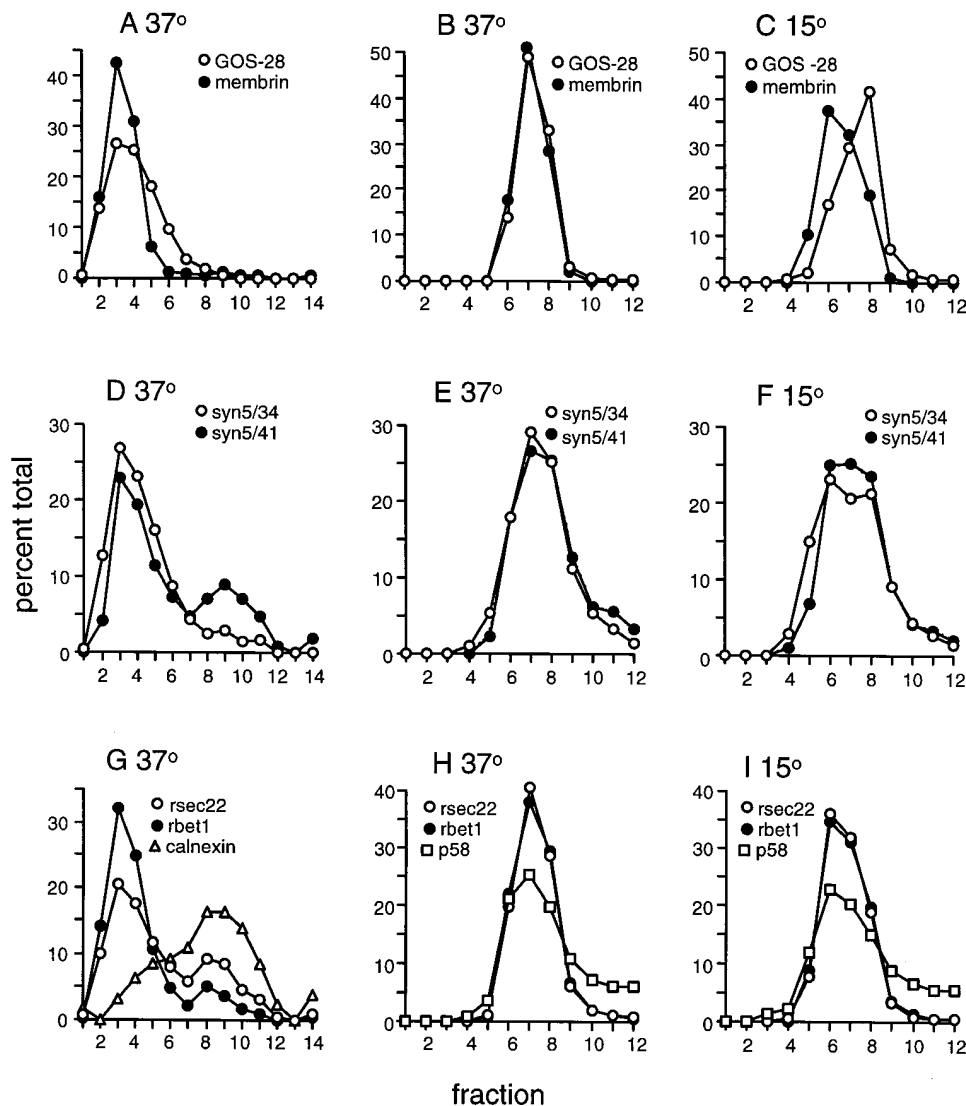


**Figure 8.** Localization and dynamics of ER/Golgi SNAREs by subcellular fractionation. NRK cells were incubated at 37°C or 15°C for 2 h, and were then homogenized and fractionated on sucrose equilibrium density gradients. (A, D, G) 0.75–1.75 M sucrose gradients that resolve Golgi/IC membranes (fractions 2, 3, and 4) from ER membranes (fractions 8, 9, and 10). Material that pelleted during centrifugation is included with fraction 14. (B, C, E, F, H, I) 0.75–1.125 M sucrose gradients that partially resolve Golgi and IC membranes at 15°C. On these shallow gradients, ER membranes pellet and are not included above. Gradient fractions were immunoblotted to detect the indicated proteins, and the amounts of each protein were quantitated by densitometry and plotted on the ordinates above. The 41-kD and 34-kD isoforms of syntaxin 5 are presented separately in D, E, and F. Fractions are displayed from least dense to most dense.

of these proteins appear to interact directly with syntaxin 5, the number of possible distinct protein complexes is large, and more information is needed about precise individual complexes.

## Discussion

Here we document significant differences in the localization and dynamics among the set of ER/Golgi SNAREs that interact *in vitro* (Hay et al., 1997). As outlined below, the spatial and temporal differences begin to suggest modes of action for each of the proteins. Our localization data demonstrate that rsec22b and rbet1 are nearly identically distributed on membranes, and are particularly enriched in the COPII-coated membranes of ER exit sites and early IC elements, including vesicles and VTCs (Table I, Figs. 2 and 3). Our data implicate a role for these proteins on COPII vesicles that mobilize anterograde cargo from the ER, and fuse into nearby early peripheral VTCs (see our working model, Fig. 11). We often observe immunogold particles representing rsec22b and rbet1 on budding vesicles, much more often than for syntaxin 5 or

membrin. rsec22b and rbet1 may mediate fusion of the transport vesicles with VTCs by virtue of SNARE complexes involving rsec22b, rbet1, membrin, and syntaxin 5 (primarily the 41-kD isoform; see model). A complex of these four proteins could involve interaction of four helical binding domains, one contributed by each protein. This interaction would be similar to the docking/fusion complex of the synapse in principle, where four helices interact, syntaxin and VAMP each contributing one helix, and SNAP-25 contributing two. rsec22b and rbet1 appear to reside on VTC elements as they cycle between peripheral and Golgi-adjacent locations, as evidenced by the dramatic redistribution of rsec22b and rbet1 caused by low-temperature incubations (Figs. 6, 7, and 8). Their presence on VTCs near the Golgi implicates them in a second round of membrane fusion: the fusion of mature VTCs to form nascent Golgi cisternae (Fig. 11). Although both rsec22b and rbet1 appear on Golgi-centric VTCs, they are uncommon in the Golgi (Table I) and are rarely found beyond the first full Golgi cisterna. Our localization data are consistent with rsec22b and rbet1 having the strongest retrieval determinants of all the SNAREs studied here,

Table IV. Quantitative Analysis of SNARE Immunoprecipitations

Cocoprecipitated Protein	Efficiency of Coprecipitation (Arbitrary Units)					IgG
	syn5	GOS-28	rsec22b	membrin	rbet1	
syn5-41	99	30	*	25	129	*
syn5-34	230	134	*	37	128	*
syn5-31	263	70	*	50	139	*
GOS-28	139	219	*	*	46	*
rsec22b	393	27	341	95	247	*
membrin	300	*	*	1182	308	*
rbet1	106	*	*	115	1317	*

For membrin and rbet1 immunoprecipitations, numbers reflect precipitations using the membrin/2-125 and rbet1/4E11 antibodies, respectively. Data is from the experiment shown in Fig. 9. \*No specific signal detected.

which would account for their relative abundance in peripheral locations including the ER and dramatic absence in the Golgi. We previously reported that myc-rbet1 targeted to Golgi and IC membranes in COS cells (Hay et al., 1996). Since Golgi cannot be distinguished from IC mem-

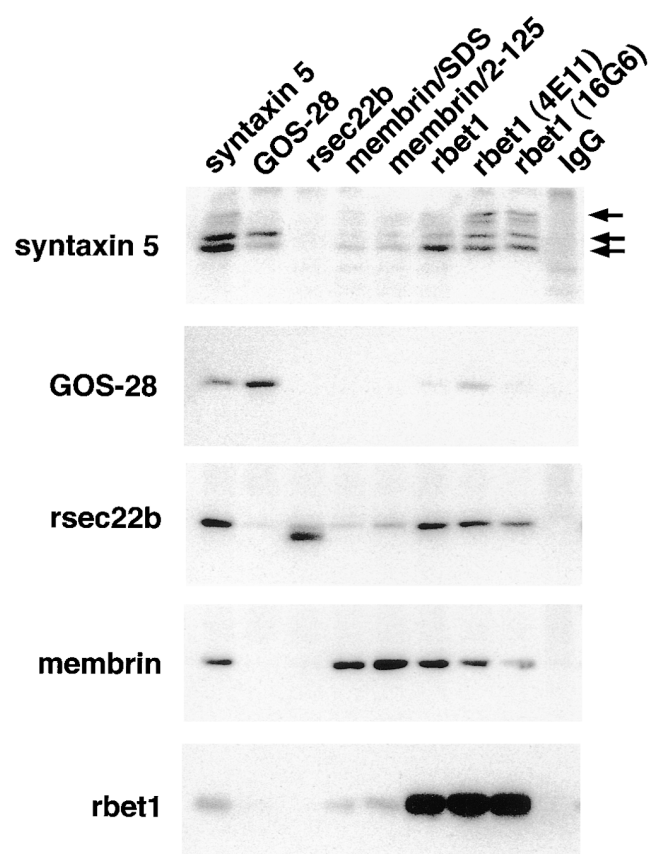


Figure 9. Syntaxin 5 isoforms immunoprecipitate in two major distinct complexes. Detergent extracts of salt-stripped rat liver membranes were subjected to immunoprecipitation using the antibodies shown along the top. The immunoprecipitates were then electrophoresed, transferred to nitrocellulose, and immunoblotted using the antibodies shown along the left. The three arrows mark the positions of the 41-kD, 34-kD, and 31-kD (degradation product of 41 kD) isoforms of syntaxin 5. Membrin/SDS rabbit antisera was prepared identically to membrin/2-125 (see Materials and Methods), except that SDS-denatured membrin was used as the immunogen.

branes at the light level, the relative distribution of the protein between Golgi and IC was not determined precisely (although we favored Golgi). The present EM study resolves that ambiguity, and indicates that very little rbet1 resides in the Golgi per se.

rsec22b and rbet1 were 2.5- to 3.5-fold more abundant on COPII-coated membrane profiles than were either syntaxin 5 or membrin (Table III). As discussed above, this fact, in conjunction with their presence in the ER (Fig. 8), implies that these two proteins function on ER-derived vesicles. However, none of the SNAREs were highly specific for COPI- vs. COPII-coated membranes. Hence, it appears that these two vesicle pathways involve highly overlapping SNARE machinery. It seems likely that all of the SNAREs examined in Table III recycle via COPI-coated membranes, and that this recycling may involve the same SNARE complexes as does anterograde transport (see model, Fig. 11). However, the interactions of SNAREs with coat protein machinery may be spatially regulated such that, for example, very early COPI vesicles would contain the majority of recycling rsec22b and rbet1, whereas later COPI vesicles in the Golgi would contain primarily syntaxin 5 and membrin. Such spatially regulated interactions could be one part of a means to prevent a seemingly random homogeneous distribution of ER/Golgi SNAREs.

Membrin is significantly less abundant in the ER (Figs. 7 and 8), less enriched in early VTCs, more enriched in Golgi-adjacent VTCs, and extends significantly further in the secretory pathway than do rsec22b and rbet1, with representation throughout the *cis* and medial Golgi (Tables I

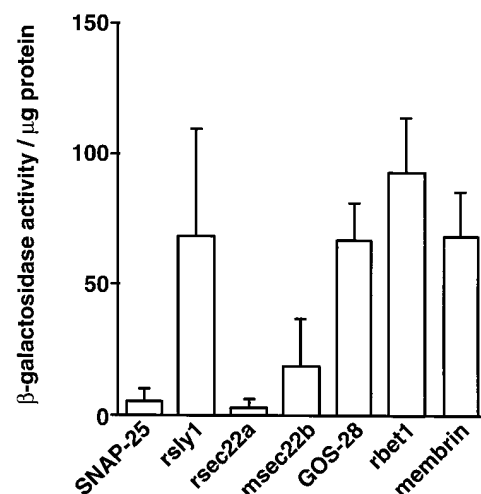
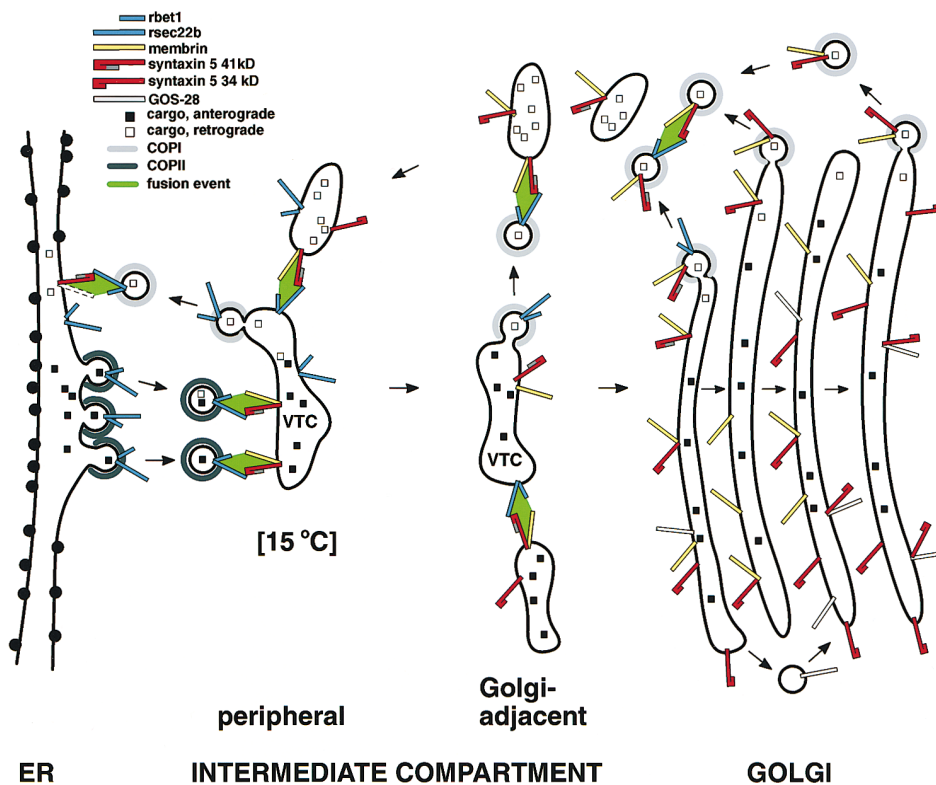


Figure 10. Multiple ER/Golgi SNAREs bind directly to syntaxin 5. HF7c reporter yeast cells were transformed with syntaxin 5 cloned into the Gal4-activation domain vector (pGAD424) in combination with different SNAREs and control proteins cloned into the Gal4-binding domain vector (pGBT9) as indicated. Transformants were allowed to grow in restrictive media, lysed, and analyzed for  $\beta$ -galactosidase activity using o-nitrophenyl- $\beta$ -D-galactoside as a substrate. Enzyme activity was expressed in arbitrary units per  $\mu$ g protein as mean value  $\pm$  SEM obtained with three independent transformants. None of the pGBT9 constructs activated  $\beta$ -galactosidase expression when tested in combination with the parental pGAD424 vector lacking a test protein insert (not shown).



**Figure 11.** Model of ER/Golgi SNARE function and trafficking. *ER/Golgi transport.* rsec22b and rbet1 bud from specialized ER exit sites on COPII-coated vesicles. These COPII-coated vesicles fuse with peripheral VTCs by virtue of SNARE complexes involving vesicle-bound rsec22b and rbet1, and VTC-bound membrin and syntaxin 5 (primarily the 41-kD isoform). Most rsec22b and rbet1 are recycled from peripheral VTCs to the ER on COPI-coated vesicles that fuse with the ER. The SNARE complex for the COPI vesicle/ER fusion is unknown, but may involve ER-localized syntaxin 5 (41-kD isoform) and possibly membrin or uncharacterized mammalian SNAREs (dashed outline, an unknown SNARE on the ER). Peripheral VTCs are the punctate intermediate observed at 15°C. At 15°C, peripheral VTCs may become enlarged and change density (not shown). Under normal conditions at 37°C, peripheral VTCs are transported along microtubules

to an accumulation of VTCs adjacent to the *cis* Golgi. Here VTCs fuse with one another and elongate to form new *cis* Golgi cisternae. This VTC/VTC fusion is mediated by SNARE complexes involving syntaxin 5 (either isoform), membrin, and remaining rsec22b and rbet1. By the time newly formed cisternae have been incorporated into the Golgi, COPI-mediated retrieval of rsec22b and rbet1, begun in the periphery, has gone to completion. COPI-dependent retrieval of membrin and the 34-kD syntaxin 5 is weaker, allowing these proteins to penetrate deeply into the Golgi stacks. Around the Golgi, retrograde COPI vesicles aggregate and fuse by virtue of vesicle-bound rsec22b, rbet1, syntaxin 5 (both isoforms), and membrin. These fusions result in larger vesicular structures (pictured) or tubules (not pictured) containing primarily retrograde cargo that is transported along microtubules to peripheral sites. Fusion of these retrograde structures with peripheral VTCs using the rsec22b/rbet1/membrin/syntaxin 5 (primarily 41 kD) SNARE complex completes the ER/Golgi transport cycle. *IntraGolgi transport.* We illustrate cisternal maturation as well as interstack vesicular transport models for completeness. Intra-Golgi transport may result from one or the other or both of these mechanisms. Golgi cisternae, initially formed by coalescence of Golgi-adjacent VTCs (see above), gradually mature as they progress from *cis* to *trans*. *cis* and medial Golgi components, e.g., resident Golgi enzymes, are maintained in their position despite maturation to later cisternae by vesicle-mediated retrograde transport (pictured above Golgi). This retrograde transport may be mediated by COPI-coated vesicles bearing recycling membrin and syntaxin 5 (both isoforms). Although these retrograde vesicles are depicted fusing only with other retrograde vesicles, they could also fuse with earlier stacks or nascent stacks of the Golgi. Rapid transport of anterograde cargo, e.g., secretory products, may be accomplished by interstack vesicle transfers (pictured below Golgi). One possibility is that interstack vesicles containing GOS-28 fuse with Golgi cisternae by virtue of a SNARE complex involving GOS-28 and the 34-kD syntaxin 5.

and II). Although membrin does not appear enriched in COPII-coated membranes (Table III), it does share residence with rsec22b and rbet1 on the peripheral VTCs that accumulate at 15°C (Figs. 6 and 7). Hence, our data is consistent with a cycling role for membrin where it would participate in fusion events between VTCs and ER-derived vesicles, as well as in later fusion of VTCs to form nascent Golgi cisternae. Membrin's extension through the Golgi suggests a role in Golgi trafficking, perhaps in addition to its presumed role in ER/Golgi transport (see Fig. 11). In fact, a recent study found functional evidence for membrin's involvement in intraGolgi trafficking (Lowe et al., 1997). Although this study did not demonstrate a role for membrin in ER-to-Golgi trafficking, the presence of membrin on rapidly cycling VTCs and its participation in protein complexes containing rsec22b and rbet1 argue for a

role in ER/Golgi trafficking. In addition, there is good evidence for involvement in ER/Golgi transport of BOS1p (Lian and Ferro-Novick, 1993), a yeast sequence homolog of membrin. Perhaps membrin's role at earlier steps is less susceptible to antibody inhibition. Although the antibody inhibition clearly demonstrated a role for membrin in Golgi trafficking, an anterograde vs. retrograde role cannot be distinguished due to the cycling nature of Golgi function.

Our data supports a dual role for syntaxin 5, like membrin, in ER/Golgi as well as intraGolgi transport. The 41-kD syntaxin 5, which is presumably more rigorously retrieved by virtue of its *N*-terminal COPI binding site (Hui et al., 1997), is more abundant in the ER and peripheral structures than the Golgi-centric form (Fig. 8). Our data is consistent with this isoform playing a role in the first fusion

event, that between ER-derived rsec22b- and rbet1-containing transport vesicles and the early VTCs (see Fig. 11). This fusion event would presumably be directed by the complex we found between the 41-kD syntaxin 5, rsec22b, rbet1, and membrin (Fig. 9, Table IV). Since the 41-kD isoform exists in the ER as well (Table I, Fig. 8), it is also possible that it functions in the fusion of COPI-mediated retrograde vesicles with the ER, perhaps as a functional analog of the yeast ER SNARE UFE1p (Lewis and Pelham, 1996) that forms a presumed retrograde SNARE complex containing SEC22p and other proteins (Lewis et al., 1997). Our localization and dynamics data are in principle consistent with a recent study documenting a functional role for syntaxin 5 at an early preGolgi stage in transport (Rowe et al., 1998). However, our data do not favor a primary role for syntaxin 5 on ER-derived transport vesicles as this report suggested. Instead we find rsec22b and rbet1 much more prevalent on these structures (Table III), implying that syntaxin 5 may serve as the vesicle receptor on the early VTC membrane (see model, Fig. 11). Later, as the VTC migrates and matures, syntaxin 5 may participate in intra-VTC fusion that may form new Golgi cisternae, an event also perhaps involving the syntaxin 5/rsec22b/rbet1/membrin complex.

The 34-kD syntaxin 5 isoform, on the other hand, is more abundant in the Golgi and Golgi-adjacent VTCs (Fig. 8). In contrast to previous ultrastructural studies localizing syntaxin 5 to Golgi-adjacent VTCs and *cis* Golgi (Banfield et al., 1994), we find syntaxin 5 immunogold particles nearly equally distributed throughout the Golgi stacks (Table III). In support of a special role for the 34-kD isoform of syntaxin 5 in Golgi trafficking, we have documented a pool of 34-kD syntaxin 5 molecules that associates with GOS-28 in a complex that lacks or excludes the dynamic SNAREs membrin, rsec22b, and rbet1 (Fig. 9, Table IV). We speculate that this complex could serve to anchor a pool of the 34-kD syntaxin 5 in the Golgi, could regulate participation of syntaxin 5 in docking interactions with other SNAREs, or could provide a basis for intraGolgi vesicle/cisternae fusions. In each of these possible capacities, the syntaxin 5/GOS-28 complex would occur within the Golgi, since our studies indicate that GOS-28 and a portion of syntaxin 5 molecules do not travel on VTCs moving between peripheral and Golgi-adjacent locations (Figs. 6 and 8). It is tempting to speculate (see Fig. 11) that the syntaxin 5/GOS-28 complex represents a docking complex between Golgi-derived vesicles containing GOS-28 and Golgi cisternae containing 34-kD syntaxin 5. This possibility would be consistent with a previous report localizing recombinant GOS-28 to Golgi rim vesicles, and demonstrating an inhibitory effect of GOS-28 antisera on intraGolgi transport (Nagahama et al., 1996). It would also be consistent with the finding that overexpression of truncated syntaxin 5 weakly inhibited intraGolgi as well as ER-to-Golgi VSV G protein transport (Dascher et al., 1994). The data seems less consistent with the proposed role for GOS-28 in ER to Golgi transport (Subramaniam et al., 1996; Hay et al., 1997).

We (Hay et al., 1997; this report, Fig. 9) and others (Lowe et al., 1997) have observed coprecipitation of rsec22b with GOS-28 and coprecipitation of GOS-28 with rbet1, but these are on a molar basis minor compared with

the major complexes described above. One of the anti-rbet1 antibodies, 4E11, coprecipitated significantly more GOS-28 than the other two rbet1 antisera; however, even in this most efficient precipitation the amount of associated GOS-28 was less than 19% of the associated rsec22b, membrin, or syntaxin 5. These relatively minor GOS-28-rbet1 interactions may arise from lateral associations of distinct SNARE complexes, or may represent intermediates in the transition between the major complexes. For example, although the function of GOS-28 with syntaxin 5 may not depend upon the presence of rbet1 (and vice versa), GOS-28 and rbet1 may not bind to syntaxin 5 in a strictly mutually exclusive manner, allowing some overlap between the major complexes to occur. Such overlap complexes could potentially serve a spatially defined regulatory purpose.

How does intraGolgi traffic work? Unfortunately, defining the distribution of SNAREs through the Golgi does not uniquely favor any one model of intraGolgi transport, including vesicle transport, cisternal maturation, and interstack tubules (Pelham, 1998; Mironov et al., 1998). For example, interstack vesicle transport throughout the Golgi could be mediated by syntaxin 5 (34 kD) and GOS-28 alone. There is no need for distinct t-SNAREs on each stack as long as spatial regulation or polarity is provided by other mechanisms such as microtubules or the Golgi spectrin/ankyrin cytoskeleton (Devarajan et al., 1997; Burkhardt et al., 1997). For completeness, the model shown in Fig. 11 incorporates nonmutually exclusive elements of cisternal maturation as well as interstack vesicle transport. It is possible that rsec22b, rbet1, syntaxin 5, membrin, GOS-28, and perhaps ykt6 (McNew et al., 1997) provide sufficient SNARE machinery to direct cargo from the ER all the way through to the TGN where cargo is sorted into one of several major pathways leading to destinations within the cell or without.

Though a complete picture of ER-to-Golgi and intraGolgi trafficking are not available, we now have enough information about the localization, dynamics, and interactions among ER/Golgi SNAREs to begin formulating useful models and specific testable hypotheses. Syntaxin 5 is likely to emerge from future studies as a common component of several spatially distinct membrane fusion complexes critical for early steps in the secretory pathway. Understanding the composition, regulation, and integration of these complexes with rabs, sec1 proteins, and membrane coat systems will provide the basis for a firm understanding of how cells mobilize and traffic their products.

We are indebted to Dr. Andy Bean (University of Texas-Houston Health Sciences Center) for technical training and advice on the yeast two-hybrid system, and for the gift of the pGAD-syntaxin 5 construct. We also wish to thank Dr. Keith Mostov (University of California-San Francisco) for the suggestion that a syntaxin 5-membrin-rsec22b-rbet1 complex could involve four SNARE binding domains, as does the synaptic ternary complex where SNAP-25 contributes two such domains.

Received for publication 15 April 1998 and in revised form 18 May 1998.

#### References

- Banfield, D.K., M.J. Lewis, C. Rabouille, G. Warren, and H.R. Pelham. 1994. Localization of Sed5, a putative vesicle targeting molecule, to the *cis*-Golgi network involves both its transmembrane and cytoplasmic domains. *J. Cell Biol.* 127:357-371.

- Bannykh, S.I., T. Rowe, and W.E. Balch. 1996. The organization of endoplasmic reticulum export complexes. *J. Cell Biol.* 135:19–35.
- Bennett, M.K., J.E. Garcia-Ararras, L.A. Elferink, K. Peterson, A.M. Fleming, C.D. Hazuka, and R.H. Scheller. 1993. The syntaxin family of vesicular transport receptors. *Cell.* 74:863–873.
- Bennett, M.K., and R.H. Scheller. 1993. The molecular machinery for secretion is conserved from yeast to neurons. *Proc. Natl. Acad. Sci. USA.* 90:2559–2563.
- Burkhardt, J.K., C.J. Echeverri, T. Nilsson, and R.B. Vallee. 1997. Overexpression of the dynamin (p50) subunit of the dynactin complex disrupts dynein-dependent maintenance of organelle distribution. *J. Cell Biol.* 139:469–484.
- Cosson, P., and F. Letourneur. 1997. Coatamer (COPI)-coated vesicles: role in intracellular transport and protein sorting. *Curr. Opin. Cell Biol.* 9:484–487.
- Dascher, C., J. Matteson, and W.E. Balch. 1994. Syntaxin 5 regulates endoplasmic reticulum to Golgi transport. *J. Biol. Chem.* 269:29363–29366.
- Dascher, C., and W.E. Balch. 1996. Mammalian Sly1 regulates syntaxin 5 function in endoplasmic reticulum to Golgi transport. *J. Biol. Chem.* 271:15866–15869.
- Devarajan, P., P.R. Stabach, M.A. De Matteis, and J.S. Morrow. 1997. Na, K-ATPase transport from endoplasmic reticulum to Golgi requires the Golgi spectrin-ankyrin G119 skeleton in Madin Darby canine kidney cells. *Proc. Natl. Acad. Sci. USA.* 94:10711–10716.
- Duden, R., G. Griffiths, R. Frank, P. Argos, and T.E. Kreis. 1991. Beta-COP, a 110 kd protein associated with non-clathrin-coated vesicles and the Golgi complex, shows homology to beta-adaptin. *Cell.* 64:649–665.
- Hammond, C., and A. Helenius. 1994. Quality control in the secretory pathway: retention of a misfolded viral membrane glycoprotein involves cycling between the ER, intermediate compartment, and Golgi apparatus. *J. Cell Biol.* 126:41–52.
- Hardwick, K.G., and H.R.B. Pelham. 1992. SED5 encodes a 39-kD integral membrane protein required for vesicular transport between the ER and Golgi complex. *J. Cell Biol.* 119:513–521.
- Harlow, E., and D. Lane. 1988. *Antibodies: A Laboratory Manual.* Cold Spring Harbor Laboratory Press, Plainview, NY.
- Hay, J.C., H. Hirling, and R.H. Scheller. 1996. Mammalian vesicle trafficking proteins of the endoplasmic reticulum and Golgi. *J. Biol. Chem.* 271:5671–5679.
- Hay, J.C., D.S. Chao, C.S. Kuo, and R.H. Scheller. 1997. Protein interactions regulating vesicle transport between the endoplasmic reticulum and Golgi apparatus in mammalian cells. *Cell.* 89:149–158.
- Hayashi, T., H. McMahon, S. Yamasaki, T. Binz, Y. Hata, T.C. Sudhof, and H. Niemann. 1994. Synaptic vesicle membrane fusion complex: action of clostridial neurotoxins on assembly. *EMBO (Eur. Mol. Biol. Organ.) J.* 13: 5051–5061.
- Hui, N., N. Nakamura, B. Sönnichsen, D. Shima, T. Nilsson, and G. Warren. 1997. An isoform of the Golgi t-SNARE, syntaxin 5, with an endoplasmic reticulum retrieval signal. *Mol. Biol. Cell.* 8:1777–1787.
- Kuehn, M., and R. Schekman. 1997. COPII and secretory cargo capture into transport vesicles. *Curr. Opin. Cell Biol.* 9:477–483.
- Kuehn, M.J., J.M. Herrmann, and R. Schekman. 1998. CopII-cargo interactions direct protein sorting into ER-derived transport vesicles. *Nature.* 391:187–190.
- Kuismanen, E., and J. Saraste. 1989. Low temperature-induced transport blocks as tools to manipulate membrane traffic. *Methods Enzymol.* 32:257–274.
- Letourneur, F., E.C. Gaynor, S. Hennecke, C. Démolière, R. Duden, S.D. Emr, H. Riezman, and P. Cosson. 1994. Coatamer is essential for retrieval of dilysine-tagged proteins to the endoplasmic reticulum. *Cell.* 79:1199–1207.
- Lewis, M.J., and H.R. Pelham. 1996. SNARE-mediated retrograde traffic from the Golgi complex to the endoplasmic reticulum. *Cell.* 85:205–215.
- Lewis, M.J., J.C. Rayner, and H.R. Pelham. 1997. A novel SNARE complex implicated in vesicle fusion with the endoplasmic reticulum. *EMBO (Eur. Mol. Biol. Organ.) J.* 16:3017–3024.
- Lian, J.P., and S. Ferro-Novick. 1993. Bos1p, an integral membrane protein of the endoplasmic reticulum to Golgi transport vesicles, is required for their fusion competence. *Cell.* 73:735–745.
- Liou, W., H.J. Geuze, and J.W. Slot. 1996. Improving structure of cryosections for immunogold labeling. *Histochem. Cell Biol.* 106:41–48.
- Lowe, S.L., F. Peter, V.N. Subramaniam, S.H. Wong, and W. Hong. 1997. A SNARE involved in protein transport through the Golgi apparatus. *Nature.* 389:881–884.
- Matlin, K.S., and K. Simons. 1983. Reduced temperature prevents transfer of a membrane glycoprotein to the cell surface but does not prevent terminal glycosylation. *Cell.* 34:233–243.
- McNew, J.A., M. Sogaard, N.M. Lampen, S. Machida, R.R. Ye, L. Lacomis, P. Tempst, J.E. Rothman, and T.H. Sollner. 1997. Ykt6p, a prenylated SNARE essential for endoplasmic reticulum-Golgi transport. *J. Biol. Chem.* 272: 17776–17783.
- Mironov, A. Jr., A. Luini, and A. Mironov. 1998. A synthetic model of intra-Golgi traffic. *FASEB J.* 12:249–252.
- Nagahama, M., L. Orci, M. Ravazzola, M. Amherdt, L. Lacomis, P. Tempst, J.E. Rothman, and T.H. Söllner. 1996. A v-SNARE implicated in intra-Golgi transport. *J. Cell Biol.* 133:507–516.
- Orci, L., M. Stames, M. Ravazzola, M. Amherdt, A. Perrelet, T.H. Söllner, and J.E. Rothman. 1997. Bidirectional transport by distinct populations of COPI-coated vesicles. *Cell.* 90:335–349.
- Paek, I., L. Orci, M. Ravazzola, H. Erdjument-Bromage, M. Amherdt, P. Tempst, T.H. Söllner, and J.E. Rothman. 1997. ERS-24, a mammalian v-SNARE implicated in vesicle traffic between the ER and the Golgi. *J. Cell Biol.* 137: 1017–1028.
- Pelham, H.R.B. 1998. Getting through the Golgi complex. *Trends Cell Biol.* 8:45–49.
- Peterson, M.R., S.C. Hsu, and R.H. Scheller. 1996. A mammalian homologue of SL1, a yeast gene required for transport from endoplasmic reticulum to Golgi. *Gene.* 169:293–294.
- Pevsner, J., S.C. Hsu, J.E. Braun, N. Calakos, A.E. Ting, M.K. Bennett, and R.H. Scheller. 1994. Specificity and regulation of a synaptic vesicle docking complex. *Neuron.* 13:353–361.
- Presley, J.F., N.B. Cole, T.A. Schroer, K. Hirschberg, K.J.M. Zaal, and J. Lippincott-Schwartz. 1997. ER-to-Golgi transport visualized in living cells. *Nature.* 389:81–85.
- Rose, M., and D. Botstein. 1983. Construction and use of gene fusions with *lacZ* which are expressed in yeast. *Methods Enzymol.* 101:167–180.
- Rowe, T., M. Aridor, J.M. McCaffery, H. Plutner, C. Nuoffer, and W.E. Balch. 1996. COPII vesicles derived from mammalian endoplasmic reticulum microsomes recruit COPI. *J. Cell Biol.* 135:895–911.
- Rowe, T., C. Dascher, S. Bannykh, H. Plutner, and W.E. Balch. 1998. Role for vesicle-associated syntaxin 5 in the assembly of pre-Golgi intermediates. *Science.* 279:696–700.
- Sacher, M., S. Stone, and S. Ferro-Novick. 1997. The synaptobrevin-related domains of Bos1p and Sec22p bind to the syntaxin-like region of Sed5p. *J. Biol. Chem.* 272:17134–17138.
- Scales, S.J., R. Pepperkok, and T.E. Kreis. 1997. Visualization of ER-to-Golgi transport in living cells reveals a sequential mode of action for COPII and COPI. *Cell.* 90:1137–1148.
- Saraste, J., and K. Svensson. 1991. Distribution of the intermediate elements operating in ER to Golgi transport. *J. Cell Science.* 100:415–430.
- Schekman, R., and I. Mellman. 1997. Does COPI go both ways? *Cell.* 90:197–200.
- Schiestl, R.H., and R.D. Gietz. 1989. High efficiency transformation of intact cells using single stranded nucleic acids as a carrier. *Curr. Genet.* 16:339–346.
- Slot, J.W., H.J. Geuze, S. Gjengack, G.E. Lienhard, and D.E. James. 1991. Immunolocalization of the insulin regulatable glucose transporter in brown adipose tissue of the rat. *J. Cell Biol.* 113:123–135.
- Søgaard, M., K. Tani, R.R. Ye, S. Geromanos, P. Tempst, T. Kirchhausen, J.E. Rothman, and T. Söllner. 1994. A rab protein is required for the assembly of SNARE complexes in the docking of transport vesicles. *Cell.* 78:937–948.
- Sollner, T., S.W. Whiteheart, M. Brunner, H. Erdjument-Bromage, S. Geromanos, P. Tempst, and J.E. Rothman. 1993. SNAP receptors implicated in vesicle targeting and fusion. *Nature.* 362:318–324.
- Stone, S., M. Sacher, Y. Mao, C. Carr, P. Lyons, A.M. Quinn, and S. Ferro-Novick. 1997. Bet1p activates the v-SNARE Bos1p. *Mol. Biol. Cell.* 8:1175–1181.
- Subramaniam, V.N., J. Krijnse-Locker, B.L. Tang, M. Ericsson, A.R. Yusoff, G. Griffiths, and W. Hong. 1995. Monoclonal antibody HFD9 identifies a novel 28 kDa integral membrane protein on the cis-Golgi. *J. Cell Sci.* 108: 2405–2414.
- Subramaniam, V.N., F. Peter, R. Philp, S.H. Wong, and W. Hong. 1996. GS28, a 28-kilodalton Golgi SNARE that participates in ER-Golgi transport. *Science.* 272:1161–1163.
- Tang, B.L., F. Peter, J. Krijnse-Locker, S.H. Low, G. Griffiths, and W. Hong. 1997. The mammalian homolog of yeast Sec13p is enriched in the intermediate compartment and is essential for protein transport from the endoplasmic reticulum to the Golgi apparatus. *Mol. Cell Biol.* 17:256–266.
- Weber, T., B.V. Zemelman, J.A. McNew, M.G. Westerman, F. Pariati, T.H. Söllner, and J.E. Rothman. 1998. SNAREpins: minimal machinery for membrane fusion. *Cell.* 92:759–772.
- Zhang, T., S.H. Wong, B.L. Tang, Y. Xu, F. Peter, V.N. Subramaniam, and W. Hong. 1997. The mammalian protein (rbt1) homologous to yeast Bet1p is primarily associated with the pre-Golgi intermediate compartment and is involved in vesicular transport from the endoplasmic reticulum to the Golgi apparatus. *J. Cell Biol.* 139:1157–1168.